

## ARTICLE

# Zebrafish blastomere screen identifies retinoic acid suppression of *MYB* in adenoid cystic carcinoma

Joseph Mandelbaum<sup>1</sup>, Ilya A. Shestopalov<sup>1</sup>, Rachel E. Henderson<sup>1</sup>, Nicole G. Chau<sup>2</sup>, Birgit Knoechel<sup>2,3</sup>, Michael J. Wick<sup>4</sup>, and Leonard I. Zon<sup>1</sup> 

Pluripotent cells have been used to probe developmental pathways that are involved in genetic diseases and oncogenic events. To find new therapies that would target *MYB*-driven tumors, we developed a pluripotent zebrafish blastomere culture system. We performed a chemical genetic screen and identified retinoic acid agonists as suppressors of *c-myb* expression. Retinoic acid treatment also decreased *c-myb* gene expression in human leukemia cells. Translocations that drive overexpression of the oncogenic transcription factor *MYB* are molecular hallmarks of adenoid cystic carcinoma (ACC), a malignant salivary gland tumor with no effective therapy. Retinoic acid agonists inhibited tumor growth in vivo in ACC patient-derived xenograft models and decreased *MYB* binding at translocated enhancers, thereby potentially diminishing the *MYB* positive feedback loop driving ACC. Our findings establish the zebrafish pluripotent cell culture system as a method to identify modulators of tumor formation, particularly establishing retinoic acid as a potential new effective therapy for ACC.

## Introduction

Pluripotent cells can be directed to differentiate in vitro for disease modeling, tumorigenesis studies, and drug screening (Cohen and Melton, 2011). However, directed differentiation protocols can be lengthy and laborious, and are thus not amenable to high-throughput screening. Image-based chemical screening using cultured zebrafish blastomere pluripotent cells establishes a system that can be used in a high-throughput fashion and takes advantage of chemical genetics approaches with zebrafish. Here, we used this zebrafish embryo cell culture system to screen for modulators of *c-myb:GFP*-expressing cell populations maintained within heterogeneous cultures. Identifying chemical suppressors could provide new therapies for tumors driven by *MYB*, thereby demonstrating the benefits of this pluripotent zebrafish embryo cell culture to understand and exploit oncogenic regulatory networks and for assays of tumor formation in various experimental settings.

Adenoid cystic carcinoma (ACC) is a malignant neoplasm arising from secretory glands, commonly the salivary glands in the head and neck, and is characterized by slow and unpredictable growth that is often fatal (Coca-Pelaz et al., 2015). ACC has a propensity to spread along nerve fibers and metastasize to other locations in the body. Recurrent *MYB* translocations have been identified in the majority of ACCs, which are characterized by overexpression of *MYB* and *MYB* targets (Persson et al., 2009; Ho et al., 2013; Mitani et al., 2016). *MYB* is a master transcrip-

tion factor with roles in proliferation and differentiation (Oh and Reddy, 1999), and many of the ACC translocations involve another transcription factor, NFIB (Ho et al., 2013). Alterations in *MYB* have been implicated in a variety of cancers, including leukemia, pediatric gliomas, and cancers of the colon, breast, and prostate (Ramsay and Gonda, 2008). ACC-specific *MYB* translocations have been recently shown to promote transformation in genetically engineered mouse models (Mikse et al., 2016).

Despite aggressive multimodality management, approximately half of ACC patients develop distant metastases, and up to one third die within two years of diagnosis (Conley and Dingman, 1974; Spiro, 1997; Bradley, 2004; Bobbio et al., 2008). No standard systemic chemotherapy regimen or approved drug therapy exists for recurrent or metastatic ACC, and no drug therapy has demonstrated either survival or a progression-free survival benefit. Whole exome sequencing of ACC tumors has revealed mutations in NOTCH and fibroblast growth factor signaling and chromatin remodeling genes, which could serve as potential therapeutic targets (Hickman et al., 1984; Stephens et al., 2013; Ross et al., 2014). However, >30 phase II clinical trials since 1985 involving cytotoxic therapy or targeted therapies against c-Kit, epidermal growth factor receptor, fibroblast growth factor receptor, and mammalian target of rapamycin, among others, have not been successful (Yarbrough et al., 2016). Activation of NOTCH1 mutations occurs in ~15% of ACCs (Ferrarotto et al., 2017), limiting

<sup>1</sup>Stem Cell Program and Division of Hematology/Oncology, Boston Children's Hospital and Dana-Farber Cancer Institute, Howard Hughes Medical Institute, Harvard Stem Cell Institute, Harvard Medical School, Boston, MA; <sup>2</sup>Department of Medical Oncology, Dana-Farber Cancer Institute, Boston, MA; <sup>3</sup>Broad Institute of MIT and Harvard, Harvard Medical School, Boston, MA; <sup>4</sup>South Texas Accelerated Research Therapeutics, San Antonio, TX.

Correspondence to Leonard I. Zon: [zon@enders.tch.harvard.edu](mailto:zon@enders.tch.harvard.edu).

© 2018 Mandelbaum et al. This article is distributed under the terms of an Attribution–Noncommercial–Share Alike–No Mirror Sites license for the first six months after the publication date (see <http://www.rupress.org/terms/>). After six months it is available under a Creative Commons License (Attribution–Noncommercial–Share Alike 4.0 International license, as described at <https://creativecommons.org/licenses/by-nc-sa/4.0/>).

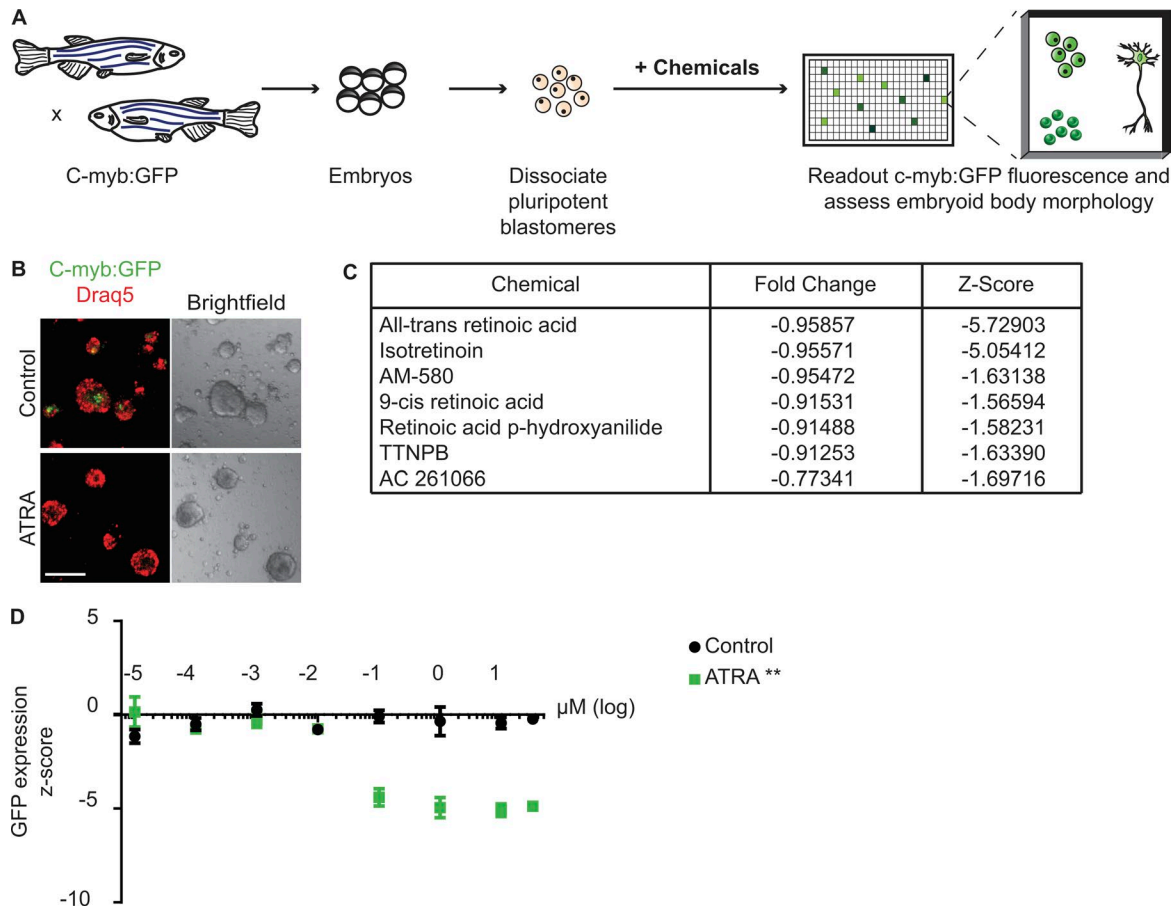


**Figure 1. Chemical genetic screen identifies retinoic acid agonists as down-regulators of *c-myb:GFP*.** (A) Schematic of a high-throughput image-based chemical screening assay. *C-myb:GFP* transgenic embryos were collected and dissociated at sphere stage. Resulting pluripotent blastomere cells were plated into 384-well plates with chemicals in duplicate. After 2 d, the 384-well plates were imaged using a Yokogawa Cell Voyager 7000 and analyzed. (B) Sample images from the screen. Hits were visually inspected for normal embryoid body formation as an indicator for toxicity. (C and D) Retinoic acid agonists decreased GFP signal in the blastomere embryo culture screen and were confirmed by dose-response curves ( $n = 4$ ). \*\* $P < 0.01$  by unpaired two-tailed Student's *t* test; mean with SEM (D). Scale bar, 50  $\mu\text{m}$ . Refer to Fig. S1.

the therapeutic use of Notch inhibitors. Hence, targeting *MYB* represents a desperately needed therapeutic strategy that has the potential to elicit broad clinical activity across many ACC tumors.

There was evidence that retinoic acid receptor (RAR) signaling inactivated the function of MYB proteins, and regulatory mechanisms were proposed, including through a physical inhibitory interaction (Boise et al., 1992; Smarda et al., 1995; Pfitzner et al., 1998; Zemanová and Smarda, 1998; Lutz et al., 2001). However, mechanistic studies of RAR regulation of *MYB*-driven cancers, such as ACC, in which enhancer regions are juxtaposed to the *MYB* locus, have been lacking. We report the first application of *MYB*-directed therapy for patients with ACC. In addition, we performed our mechanistic studies, including our chromatin immunoprecipitation sequencing (ChIP-seq) analysis, directly on patient-derived human ACC tumors to establish our model of tumor inhibition.

Here, through a transgenic zebrafish embryo cell culture screening approach, we identified retinoic acid agonists as potent suppressors of *c-myb:GFP* fluorescence. We showed that all-trans retinoic acid (ATRA) decreases *c-myb*<sup>+</sup> hematopoietic stem and progenitor cells (HSPCs) in live transgenic zebrafish

embryos and by in situ hybridization, but has no effect on differentiated myeloid cell populations. We treated human U937 cells with various retinoic acid agonists and observed a rapid decrease in *c-myb* levels, which showed that retinoic acid suppressed *c-myb* expression through transcriptional regulation. We were interested in applying retinoic acid agonists to ACC models. ATRA and isotretinoin slowed tumor growth in ACC primagraft models in vivo and diminished *MYB*-bound translocated enhancers. We observed physical binding of RAR at the *MYB* locus, consistent with our model of retinoic acid-induced transcriptional suppression of *MYB*. Thus, our work establishes the preclinical activity of ATRA and other retinoic acid agonists in ACC and will lead to a clinical trial shortly.

## Results

### Zebrafish chemical genetic screen identifies regulators of *c-myb* expression

We previously reported a chemical genetic screen that identified inducers of myogenesis using an embryonic pluripotent blastomere culture system in zebrafish (Xu et al., 2013). Here,

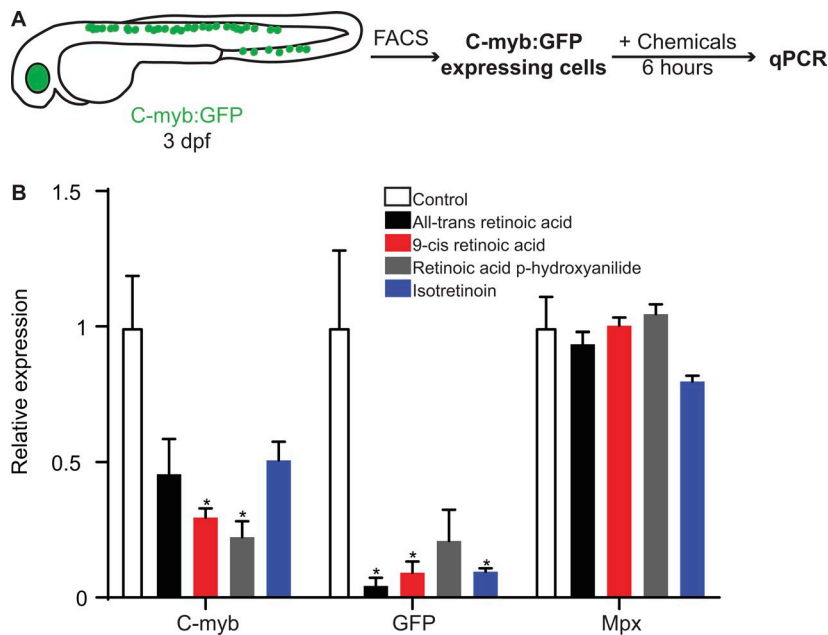


**Figure 2. Retinoic acids down-regulate endogenous *c-myb* expression in *c-myb:GFP*-expressing cells. (A)** Schematic of *c-myb:GFP*-positive cells were sorted from 3-d postfertilization (dpf) transgenic embryos, plated with chemicals for 6 h, and analyzed by quantitative PCR (qPCR). **(B)** Expression of genes after retinoic acid agonist treatment shown relative to control cells ( $n = 3$ ). \* $P < 0.05$  by unpaired two-tailed Student's *t* test; mean with SEM. Mpx, myeloperoxidase (a neutrophil marker).

we have adapted this culture screening system to find modulators of *c-myb*, a marker of HSPCs. We used a culture system involving a BAC transgenic reporter with GFP at the ATG of the *c-myb* gene (North et al., 2007). Embryos were dissociated into single cells at sphere stage (4 h postfertilization [hpf]) and plated with chemicals for 2 d until fluorescence was evaluated (Fig. 1 A). Gene expression analysis of sorted *c-myb:GFP*-expressing cells demonstrated that these cells derived in culture contained a mixture of blood, neuroepithelial, and retinal cell types, thereby proving that *c-myb:GFP* was expressed in similar tissues as the endogenous gene in zebrafish.

We screened 3,840 bioactive small molecules in duplicate for suppression of *c-myb:GFP* and identified 107 chemical hits (2.8% hit rate,  $z$ -score  $< 1.44$ , and  $> 70\%$  *c-myb:GFP* down-regulation). The  $z$ -score represents the average across the two plates and normalizes for variable amounts of GFP fluorescence among the plates screened. Visual inspection revealed that 22 hits had normal embryoid body formation (Table S1). This suggested that the *c-myb:GFP* down-regulation observed was specific and not due to toxicity effects of the chemicals (Fig. 1 B), as opposed to the remaining hits that showed poor embryoid body morphology indicative of general cell toxicity. Retinoic acid agonists were identified as potent suppressors of *c-myb:GFP* expression in the blastomere cultures at low concentrations (Fig. 1, C and D; and Fig. S1). Given that *c-myb:GFP* was expressed by a variety of different cell types in the culture system, the retinoic acid effects on *c-myb* expression can occur in many tissues.

#### Retinoic acid agonists decrease *c-myb*-positive cells in vivo

*C-myb* is required for HSPC formation in zebrafish and mammalian blood development (Orkin and Zon, 2008). *C-myb* is also expressed in mature myeloid cells such as neutrophils and macrophages (Graf, 1992). Thus, we wanted to investigate if retinoic acid treatment functions on HSPCs and myeloid cells located in the subsequent hematopoietic niche between 48 and 72 hpf. We quantified the number of *c-myb:GFP*<sup>+</sup> cells of live

zebrafish embryos treated with ATRA in double-transgenic embryos along with *mpeg1:mCherry*<sup>+</sup> (macrophage marker) or *lyz:dsRed*<sup>+</sup> (neutrophil marker) cells at 72 hpf (Fig. S2 A). We also examined alterations on endogenous hematopoietic populations by whole mount in situ hybridization in ATRA-treated wild-type AB embryos (Fig. S2 E). In embryos treated with ATRA, we found there was a significant decrease in the number of *c-myb:GFP*<sup>+</sup> cells (Fig. S2, B–D) and *c-myb* and *runx1* expression (Fig. S2, F, G, and J). There was no significant difference in *mpeg1:mCherry*<sup>+</sup> and *lyz:dsRed*<sup>+</sup> cells (Fig. S2, B–D) or *mpx* (myeloperoxidase, a neutrophil marker) and *I-plastin* (macrophage and neutrophil marker) expression (Fig. S2, H–J). Other retinoic acid agonists besides ATRA also strongly decreased *c-myb* levels (Fig. S2 J). Taken together, these findings argue strongly for a specific inhibitory role of retinoic acid agonists on the *c-myb*-positive HSPC population that does not affect mature myeloid cells.

#### Retinoic acid agonists work rapidly to down-regulate *c-myb* expression in isolated tissues

To examine the role of retinoic acids on endogenous *c-myb* expression, we sorted *c-myb:GFP*-expressing cells from 72-hpf transgenic embryos and treated them ex vivo with 1  $\mu$ M retinoic acid agonists for 6 h (Fig. 2 A). At this stage, transgenic zebrafish express *c-myb:GFP* in blood, neural, hatching gland, and eye tissues. Retinoic acid treatments caused a rapid decline in *c-myb* and *GFP* transcript expression, whereas *mpx* gene expression was unaffected (Fig. 2 B), in accordance with our in vivo findings.

We predicted that the retinoic acid down-regulation of *c-myb* expression in zebrafish embryos and cell cultures could likewise act in mammalian tissues. Retinoic acid has been linked to a block of differentiation in certain systems, and this correlates with a reduction in *c-myb* (Thiele et al., 1988; Weston, 1990; Thompson and Ramsay, 1995). Our data that retinoic acid works very quickly to lower *c-myb* mRNA expression in isolated zebrafish cells strongly suggest a direct, rapid action of retinoic acid on the *myb* gene.

We next sought to treat human cell lines with retinoic acid and evaluate expression of *myb*. Ideally, we would directly evaluate if retinoic acid suppresses *myb* in ACC. There are no validated ACC cell lines available for in vitro analysis, and thus these experiments are not possible. A discussion with the Adenoid Cystic Carcinoma Research Foundation confirmed that there are no ACC cell lines available (unpublished data). Although some primary ACC tumors have been cultured in the short term (Almeida et al., 2017; Nör et al., 2017; Panaccione et al., 2017), these ACC cultured cells grow poorly. Hence, we tried retinoic acid treatment of human U937 cells, a myeloid leukemia line that expresses high levels of *c-myb*, to facilitate our in vitro studies. These studies were simply to prove that the *myb* suppression could be accomplished in human cells.

U937 cells down-regulated *c-myb* expression within 1 h of ATRA treatment and for extended periods of time (Fig. S3, A and B), which suggested a direct transcriptional mechanism of regulation and was consistent with previous reports (Smarda et al., 1995). We also analyzed other retinoic acid agonists that were able to decrease *c-myb* expression (Fig. S3 C). Retinoic acid binds RAR ( $\alpha$ ,  $\beta$ , or  $\gamma$ ), which exists as a heterodimer with retinoid X receptor (RXR) and acts to control gene transcription upon ligand binding (Cunningham and Duester, 2015). Although 9-*cis* retinoic acid is a natural ligand of both pan-RAR and RXR (Allenby et al., 1993), the reduction in *c-myb* gene expression we observed with the pan-RAR agonists ATRA, retinoic acid *p*-hydroxyanilide, and isotretinoin (Das et al., 2014) strongly indicated that signaling via RAR specifically was responsible for *c-myb* down-regulation. We also observed an increase in Mac1<sup>+</sup> U937 cells in response to ATRA treatment (data not shown), consistent with reports of ATRA-induced differentiation in U937 cells (Olsson and Breitman, 1982). Retinoic acid agonists inhibited U937 proliferation in a dose-dependent manner after 48 h of treatment (Fig. S3, D and E), suggesting that the acute reduction of *c-myb* and the transcriptional response to retinoic acid leads to a proliferative defect.

### Retinoic acid agonists slow ACC tumor growth in vivo

*MYB* translocations are near-universal features in ACC in which the *MYB* gene regulatory elements are maintained in the resulting fusions (Wysocki et al., 2016). The nuclear hormone receptors, including the steroid receptors, androgen receptors, and RARs, bind to a common RXR (Evans and Mangelsdorf, 2014). The binding of one ligand to RXR could therefore block the response to another ligand, essentially preventing the transactivation potential or DNA binding of the specific receptors. Hence, ATRA, as a retinoic acid agonist, could block *MYB* transcription directly, especially given the rapid inhibition in *c-myb* gene expression we observed by retinoic acid treatments. In addition, ATRA would also be an appealing drug for ACC since it is clinically available for acute promyelocytic leukemia. By decreasing transcription of the *MYB* gene, we reasoned that it may be possible to modify the course of the disease with retinoic acid treatments by disrupting positive feedback loops involving *MYB*.

We assessed the in vivo efficacy of ATRA and isotretinoin in ACC xenotransplantation trials (Fig. 3 A). Evidence suggests that patient-derived xenografts (PDXs) serve as the most reliable pre-clinical model available by preserving tumor structure and het-

erogeneity and facilitating clinical predictions of drug responses in vivo (Ruggeri et al., 2014). PDX studies are particularly important in ACC given that there are currently no ACC cell lines that can be cultured. Most ACC tumors are low grade (grades 1 and 2, with “tubular” and “cribriform” patterns, respectively), usually showing a mixture of both of these growth patterns, and are histologically dominated by myoepithelial cells, whereas a small number of tumors have predominantly luminal epithelial cells and are more aggressive (grade 3, with >30% “solid” pattern; Seethala, 2009; van Weert et al., 2015). For long-term tumor growth inhibition studies, we engrafted nude mice with three different human ACC tumors: x6 (grade 2 primagrafts) and x9 and x11 (grade 3 primagrafts). These PDX models were isolated from different patients, confirmed to have *MYB* translocations, and shown to recapitulate the parent tumors by histology and gene expression (Moskaluk et al., 2011).

Randomized groups of mice were treated with vehicle, ATRA, or isotretinoin, and tumor size was measured over time (Fig. 3 B). Retinoic acid treatment inhibited tumor growth significantly (Fig. 3 C). After long-term tumor growth studies were completed in ~28 d, we discontinued ATRA treatment and continued to measure tumor size in the ATRA-treated mice groups over an extended period of time to monitor tumor maintenance after treatment (Fig. S4 A). Available mice weight data from two of the three long-term studies are provided (Fig. S4 B). Tumor inhibition was maintained in ACC x11, but not in ACC x6 and x9, suggesting that continuous treatment is needed to target residual tumor cells.

We performed xenotransplantation studies with ACC x9 and x5M1 (grade 2 primagraft) consisting of 3-d treatment with vehicle or ATRA to examine short-term kinetic responses. We detected a decrease in *MYB* protein expression as determined by Western blot analysis in ATRA-treated long-term ACC x11 and short-term ACC x5M1 primagrafts (Fig. 3 D and Fig. S5 A). For these short-term studies, we were interested in studying x5M1 primagrafts specifically, as this ACC line was derived from a metastatic site and is generally considered to be more resistant to treatments. RAR $\alpha$  protein expression increased in the ATRA-treated samples, indicating that the tumors responded to ATRA treatment and that RAR $\alpha$  thus serves as a useful marker to monitor ATRA response.

We examined apoptosis by caspase-3 and proliferation by Ki-67 markers with immunohistochemistry in the ACC x6, x9, and x11 primagrafts at the conclusion of the long-term treatment at 28 d (Fig. 3, E and F; and Fig. S5 B). At the time points we examined, ATRA treatment appeared to cause more cell death, which could account for the marked tumor growth inhibition we observed during the xenotransplantation trial, but had no significant effect on proliferation. When ATRA treatment was discontinued (Fig. S4 A), tumor inhibition of ACC x11 was maintained, suggesting that these tumors did not regrow despite the presence of proliferative areas with Ki-67-positive cells, which is a phenomenon that has been reported in other cancers (Ottewell et al., 2010).

Translocations involving *MYB* have been previously described in ACC for bringing strong enhancers into close proximity of the *MYB* locus, and these enhancers are also bound by *MYB* protein, resulting in a positive feedback loop that drives *MYB* overexpression (Drier et al., 2016). Since there are no ACC cell lines

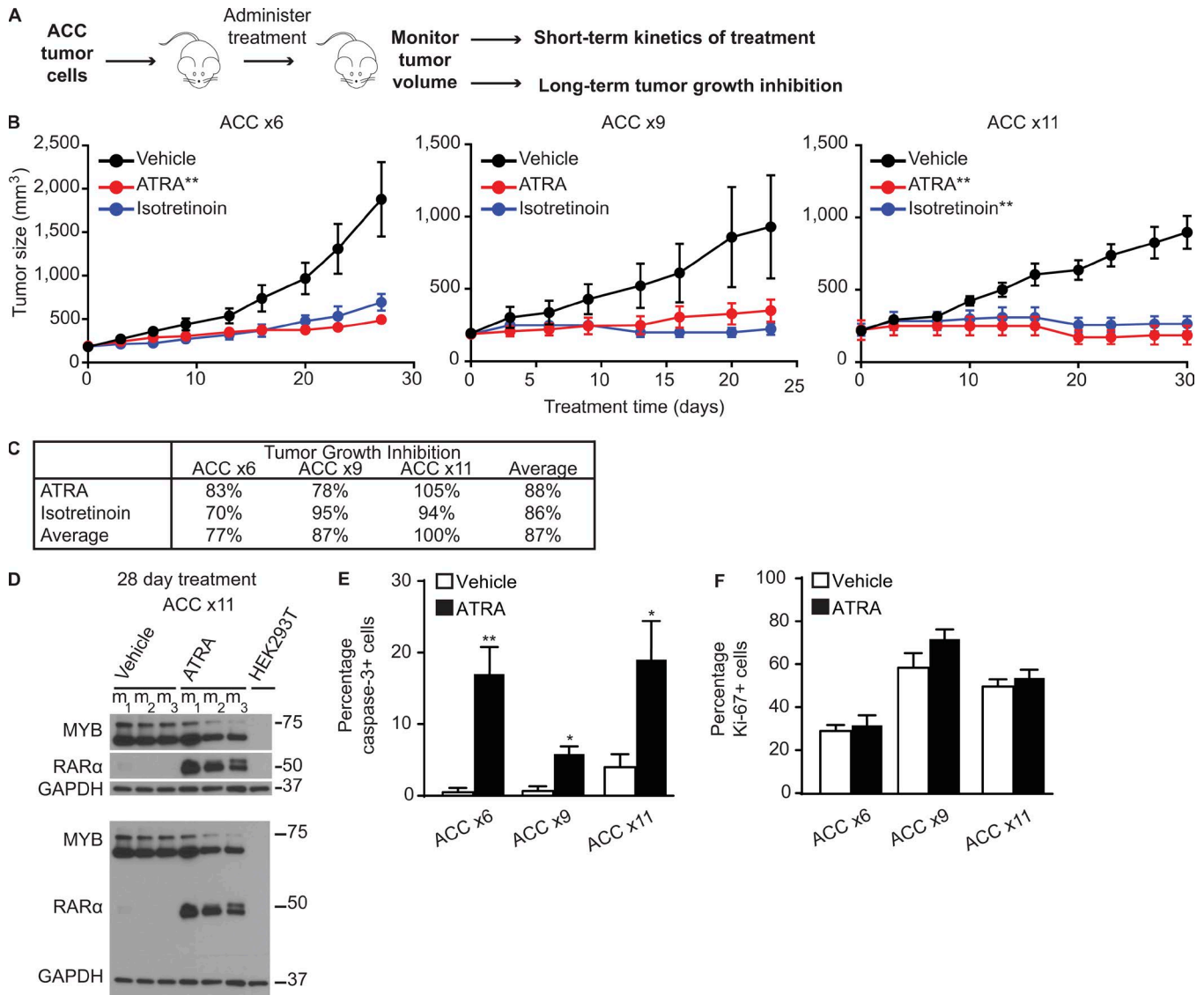


**Figure 3. Retinoic acids slow tumor growth in patient-derived ACC primgrafts. (A)** Experimental design for ACC xenotransplantation trials. **(B)** Average tumor size from four to nine nude mice (CRL: ATH/NU) per group is shown during the xenotransplantation trial period. Refer to Fig. S4. **(C)** Average final tumor growth inhibition across the different human tumors and treatments shown in B. **(D)** Protein expression of MYB and RAR $\alpha$  in individual ACC x11 primgrafts at the conclusion of the xenotransplantation trial (three primgrafts from different mice shown for each group). HEK293T cell lysate is a negative control lacking MYB expression. The full scan of the original blot is provided below the cropped sections. Size standards are in kilodaltons. Refer to Fig. S5 A. **(E and F)** Percentage of cleaved caspase-3 and Ki-67-positive nuclei was quantified from immunohistochemistry sections of primgraft tumors at the conclusion of the xenotransplantation trial ( $n = 3$  images quantified, >200 nuclei each). ATRA treatment induced more cell death in the tumors (E) but had no significant effect on proliferation (F). Refer to Fig. S5 B for representative images. \* $P < 0.05$ , \*\* $P < 0.01$  by unpaired two-tailed Student's  $t$  test; mean with SEM.

available to the scientific community, we undertook mapping of MYB protein binding in ACC x9 primgrafts by ChIP-seq after 3 d of treatment. Few articles have published ChIP-seq results from primgrafts, but we had adequate material for high quality reads. We specifically observed a strong decrease in MYB binding due to ATRA treatment at two translocated enhancers in the downstream region of *NFIB* that is fused to the *MYB* locus in ACC x9 (Fig. 4 A). In addition, there was a concomitant decrease in H3K27ac (marking active enhancers; Rivera and Ren, 2013) at these enhancer sites. ATRA treatment also resulted in a modest decrease in MYB binding at the *MYB* promoter, which would further act to weaken autoregulatory feed-forward mechanisms. Upon ATRA treatment, we found that RAR binds physically at

the 5' region of the *MYB* gene and at the translocated enhancer downstream of exon 9 of *NFIB*. We confirmed that these sites have RAR $\alpha$  binding motifs as determined by the JASPAR database (Mathelier et al., 2016).

ATRA treatment stimulated the increased expression of RAR due to positive autoregulation by the agonist-bound receptor (Fig. 5 A). Thus, RAR levels become elevated at the *MYB* promoter and enhancer (En1 in Fig. 4 A). The elevated levels of RAR on the *MYB* regulatory elements are repressive and cause a reduction in *MYB* expression. The *CEP89* gene, among others that are bound by MYB, also show this mechanism (Fig. 5 B). It is also possible that increased RAR binding displaces MYB binding, and other complex mechanisms of regulation are also possible (Pfitzner et

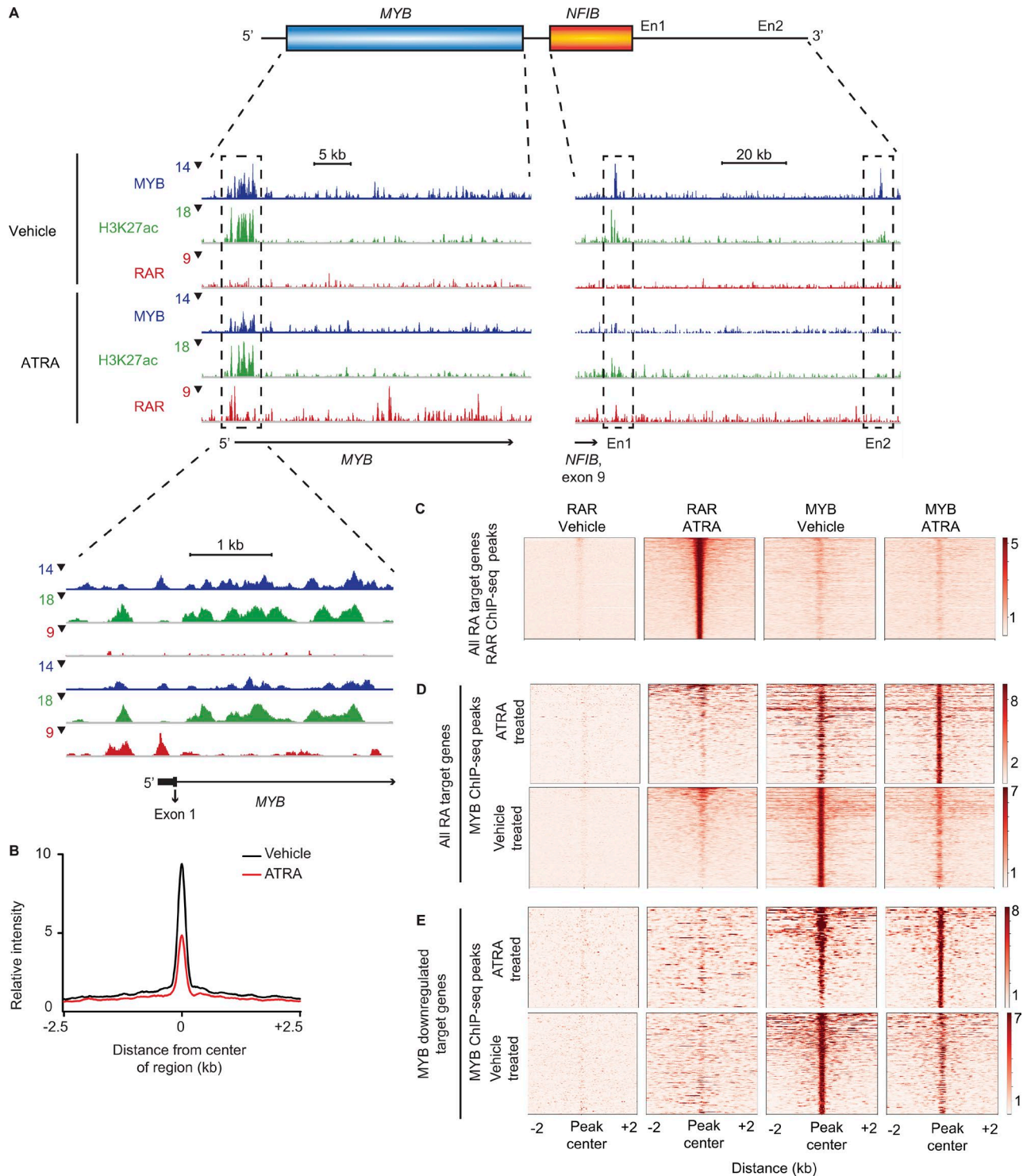


**Figure 4. Retinoic acids decrease MYB binding at translocated enhancers.** (A) Diagram illustrates the chromosomal rearrangements that maintain MYB overexpression in ACC. MYB- and RAR-binding and H3K27ac profiles are shown at the *MYB* locus or downstream of *NFIB* exon 9 in ACC x9 tumors that have *MYB-NFIB* translocations (negative strand shown). Previously described translocated MYB-bound enhancers (Drier et al., 2016) are labeled as En1 and En2. (B) MYB binding is reduced overall genome-wide in response to ATRA ( $P < 0.0001$ ). Composite enrichment profile for MYB-bound regions ( $n = 1,872$ ) normalized in ACC x9 vehicle and ATRA-treated samples. (C–E) RAR and MYB binding profile heat maps of gene sets in vehicle- or ATRA-treated patient-derived primgrafts. (C) Analysis of the RAR peaks in the ATRA-treated tumors across all retinoic acid target genes showed slight MYB binding that did not change between the vehicle- and ATRA-treated tumors. (D) Analysis of retinoic acid target genes showed overall MYB binding did not change across genes that were still MYB bound in ATRA-treated tumors, but MYB binding decreased significantly in genes that were MYB bound in the vehicle-treated tumors. (E) Genes that had a fold decrease of  $\geq 1.2$  by RNA-seq due to ATRA treatment and remained bound by MYB in ATRA-treated tumors showed no decrease in MYB binding upon ATRA induction, whereas MYB-bound genes in the vehicle-treated tumors showed decreased MYB binding upon ATRA induction. ChIP-seq peaks of the corresponding samples were assigned to genes within 15 kb. RA, retinoic acid. Refer to Fig. 5.

al., 1998; McKeown et al., 2017). Our study illustrates that disruption of the common core *MYB* circuitry in ACC with retinoic acid agonists results in RAR binding at the *MYB* gene and downstream translocated enhancers, which suppresses *MYB* binding at these regulatory sites, inhibits transcription of *MYB*, and offers a new potential therapy targeting the underlying cause of the disease.

We used ChIP-seq to identify super-enhancers from chromatin regions with high H3K27ac levels (Hnisz et al., 2013) in ACC primagraft tumors and ranked the enhancers based on enrichment (Table S2). *MYB* target genes were associated with super-enhancers, such as *EN1*, *CREB3L2*, *ITGA6*, *JAG1*, *NUFI1*, *ARID1A*, *CDH1*, *SPEN*, *NOTCH1*, and *CCND1*, as was previously observed (Drier et al., 2016). We also found that numerous super-enhancers were associated with neural crest genes (Fig. 5 C), which is consistent with reports linking ACC to drivers of neural crest cells (Yarbrough et al., 2016). These super-enhancers provide opportunities for new targets in ACC.

We determined by RNA sequencing (RNA-seq) that *RARA* and *RARG* gene levels significantly increased ~35% in short-term ACC x9 primagrafts, and *MYB* levels decreased 18% due to ATRA treatment ( $n = 3$ ,  $P < 0.05$ ). Using gene set enrichment analysis on this RNA-seq data (Subramanian et al., 2005), we found both an enrichment of *MYB* target genes (Shepard et al., 2005) and cell cycle genes (O'Farrell, 2001; Bruinsma et al., 2012; Wang et al., 2014) positively associated with vehicle-treated tumors and negatively correlated with ATRA-treated tumors, as expected (Fig. 5 D). We also discovered reduced *MYB* protein binding genome-wide due to ATRA treatment (Fig. 4 B). To determine the specific effect of *MYB* binding due to ATRA induction, we assigned ChIP-seq binding peaks to genes within 15 kb and generated heat maps around those peaks (Fig. 4, C–E). Analysis of the retinoic acid target gene set list, which includes genes that were either up-regulated or down-regulated, showed increased binding of RAR to the targets, but no correlation between *MYB* binding in the vehicle- and ATRA-treated ACC primagrafts (Fig. 4 C). We further analyzed the retinoic acid-induced gene set list to determine the effect on *MYB* binding. In this analysis of the *MYB* peaks we obtained by ChIP-seq, *MYB* binding decreased significantly in genes that were *MYB* bound in the vehicle-treated tumors, but there were no binding differences observed in the peaks of ATRA-treated tumors compared with vehicle (Fig. 4 D). The *MYB* gene is an example of the former, as it is a target of retinoic acid, and the *MYB* binding in the vehicle-treated tumors was strongly decreased upon ATRA treatment. We also analyzed *MYB* target genes that were down-regulated by ATRA induction independent of RAR binding, and similarly saw that *MYB* binding decreased significantly in genes that were *MYB* bound in the vehicle-treated tumors, but there were no binding differences observed in the peaks of ATRA-treated tumors compared with vehicle (Fig. 4 E). While there are many genes like *MYB* with reduced expression after treatment with ATRA, these data collectively support the concept that ATRA treatment leads to a specific gene program with decreased *MYB* binding in particular target genes in patient-derived primagrafts.

Our studies also show that *RAR $\alpha$*  protein levels are significantly up-regulated in the tumors treated with ATRA, with very low expression in the vehicle-treated tumors. *RAR $\alpha$*  expression

serves as a marker for tumor response to ATRA (Fig. 3 D). *RAR $\alpha$*  establishes that the tumor received retinoic acid, but does not necessarily imply that the *MYB* levels are reduced in the tumor. Nevertheless, this could help monitor the efficacy of ATRA in a planned clinical trial for metastatic ACC. Our studies suggest that ATRA acts via RAR to suppress *MYB* expression, possibly through an interruption of the *MYB*-driven regulatory loops that leads to an abrogation of the oncogenic activity of the fusion gene. Our work suggests that prolonged exposure to ATRA could be used as a treatment for ACC.

## Discussion

In this study, we used a zebrafish chemical genetic screening approach that revealed retinoic acid agonists as down-regulators of *c-myb*. Our high-throughput blastomere cell screening platform leverages the benefits of zebrafish, including the high fecundity of adults to collect thousands of embryos each week for chemical screening, and the high degree of genetic conservation with mammals for the reliable translation of chemical hits. We were able to screen thousands of compounds in an automated manner at a fraction of the time that would be needed to analyze whole embryo readouts, as in an in situ hybridization-based screen. The zebrafish screen was performed using a GFP reporter driven by the natural transcriptional regulatory elements, which revealed transcriptional suppressors of *c-myb*. Retinoic acid treatment in ACC primagrafts resulted in lower *MYB* occupancy at the 5' *MYB* regulatory element and even lower occupancy at translocated enhancers as a result of this transcriptional suppression of *MYB*. Retinoic acids identified in our zebrafish embryo cell culture strategy thus showed strong ACC tumor growth inhibition in xenotransplantation models by targeting *MYB*, which highlights the power of our zebrafish system as a preclinical discovery tool.

ACC is a fatal disease without an effective therapy. Translocated enhancers from *MYB* chromosomal rearrangements in ACC generate positive feedback loops that lead to *MYB* overexpression and malignant transformation. Here, we have found that retinoic acid causes a reduction in *c-myb* levels in zebrafish and patient-derived ACC tumors. Retinoic acid agonists are potent transcriptional suppressors of *MYB*, as RAR is physically bound at the *MYB* locus. Retinoic acid treatment causes a decrease in H3K27ac and *MYB* binding at the translocated enhancers, which can weaken the oncogenic *MYB*-driven feedback loops to cause tumor cell death.

Our function studies on the effect of retinoic acid on *MYB* expression in ACC, taken together with the clinical availability of ATRA and known toxicity profile, provide a strong rationale to treat ACC with ATRA. Acute promyelocytic leukemia due to a translocation resulting in promyelocytic leukemia/*RAR $\alpha$*  fusion can be treated with an ATRA split dose of 45 mg/m<sup>2</sup> daily (Degos and Wang, 2001). ATRA treatment is often combined in these patients with anthracycline chemotherapy or, in low-risk patients (white blood cell count <10,000/ $\mu$ l and platelet count >40,000/ $\mu$ l), with arsenic trioxide (Lo-Coco et al., 2016). The aberrant protein containing a *RAR $\alpha$*  fusion is sensitive to ATRA and is consequently degraded. Although the mechanism of action of ATRA in acute promyelocytic leukemia is distinct from the *MYB* tran-

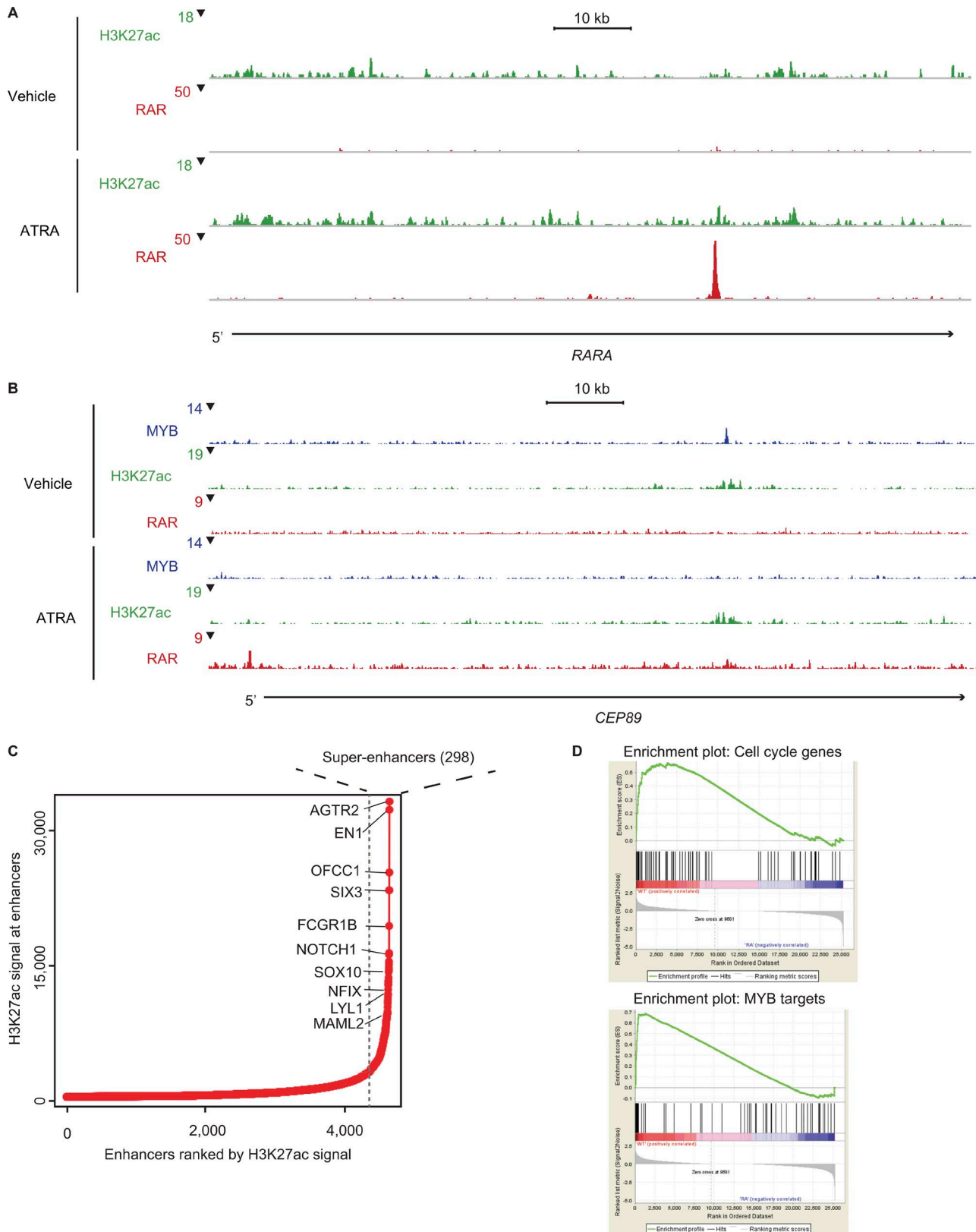


Figure 5. **Retinoic acids decrease MYB target genes in ACC primagrafts. (A and B)** Binding profiles show the positive autoregulation by the RAR upon ATRA treatment at the *RARA* locus (A) and decreased MYB binding at the *CEP89* locus (B) in response to ATRA (negative strands shown). **(C)** Super-enhancers are associated with neural crest genes. Enhancers are ranked by the amount of H3K23ac signal (x axis), and the levels of normalized H3K27ac signal is plotted (y axis) with super-enhancers above the inflection point on the curve ( $n = 298$ ). **(D)** Gene set enrichment analysis shows a positive association between cell cycle genes (top) and MYB target genes (bottom) in short-term vehicle-treated ACC x9 primagrafts and a negative correlation due to ATRA treatment (based on  $n = 3$  tumors for each condition). Related to Fig. 4 and Table S2.

scriptional inhibition we propose in ACC, the known safety profile of ATRA may guide its use in ACC. In addition, we established RAR $\alpha$  as a marker that could be used to monitor ATRA induction in biopsies from ACC patients receiving ATRA in a clinical trial. This, coupled with monitoring circulating tumor DNA for the translocation, will facilitate the correlation of tumor response to ATRA to clinical activity.

Approximately 10% of ACC tumors harbor translocations involving the related *MYBL1*, but to our knowledge there are no PDX models harboring an *MYBL1* fusion. The common oncogenic pathways in *MYB* and *MYBL1* ACC tumors were reported to be interchangeable, and the translocations often truncate the 3' specificity-conferring end of the related *MYB* and *MYBL1* (Brayer et al., 2016). These observations suggest that retinoic acid may also be therapeutically useful in ACC tumors with *MYBL1* rearrangements, which is a subject worthy of future study.

Unlike ACC x9 and x11 tumors, ACC x6 tumors are sensitive to bromodomain inhibitors (Drier et al., 2016). ACC x9 tumors are NOTCH dependent and show sensitivity to gamma-secretase inhibitors (Stoeck et al., 2014). In contrast, we observed tumor sensitivity to retinoic acids across ACC x6 (involving *MYB-TGFBR3* translocations) and x9 and x11 (both involving *MYB-NFIB* translocations) primagrafts, which shows that our strategy of targeting *MYB* can be applied effectively against different ACC mutations in grade 2 and 3 tumors. Given the near-universal prevalence of *MYB* activation in ACC tumors, the exploitation of *MYB* targeting has the potential to offer broad therapeutic efficacy. We plan to test single-dose ATRA in patients with metastatic ACC to examine safety and efficacy.

Our pluripotent blastomere culture assay enabled us to identify chemical regulators of *c-myb:GFP* expression. Virtually any zebrafish reporter line of interest can be incorporated in this versatile system, which makes it a powerful discovery tool to screen for chemical modulators of tumor formation, identify regulators of oncogenic events, perform tumor suppressor screens, and assay for new therapies to target other tumors.

## Materials and methods

### Study design

The goal of the study was to identify chemical suppressors of *MYB*. The study used a zebrafish embryo cell culture as a screening platform. Retinoic acid agonists were tested in independent *in vitro* and *in vivo* models, including human patient-derived ACC tumor xenografts in mice, U937 cells, and zebrafish. The mechanism of action of retinoic acids on *MYB* regulation and hematopoiesis was validated in the human ACC primagraft tumors, U937 cells, and zebrafish using chemical genetic and biochemical assays. Tumors from three different primary human ACC patients were used in the xenotransplantation trials and tested with vehicle, ATRA, or isotretinoin. Drug effects were measured relative to vehicle control. Mice were assigned randomly to groups. Zebrafish *in situ* staining, caudal hematopoietic tissue (CHT) cell counting, and tumor immunohistochemistry sections were scored blindly. Experiments were performed in triplicate, unless otherwise stated, data points were combined from in-

dependent biological replicates and experiments, and outliers were not excluded.

### Culture of dissociated blastomere cells

Stage-matched zebrafish blastomeres were dissociated at 4 hpf and grown in a medium composed of 5% FBS and 10% embryo extract, with the remaining 85% of medium containing 50% Leibowitz's L-15 (Invitrogen), 20% DMEM (Invitrogen), and 30% DMEM/F-12 (Invitrogen), supplemented with 2% B27 (Gibco), 15 mM Hepes (Gibco), 1% L-glutamine (Gibco), 1% N2 (Gibco), 10 nM sodium selenite (Sigma), 100  $\mu$ g/ml piperacillin (Sigma), 10  $\mu$ g/ml ciprofloxacin (GenHunter), and 0.018% sodium bicarbonate (Gibco). Embryo extract was made by homogenizing 24-hpf wild-type AB embryos in HBSS (Gibco). All zebrafish experiments and procedures were performed as per protocols approved by the Boston Children's Hospital Institutional Animal Care and Use Committee (IACUC) and the Harvard University IACUC.

### High-throughput screen

To screen each chemical library plate in duplicate, two 384-well plates were coated with 0.1% gelatin. *C-myb:GFP* (North et al., 2007) embryos were washed with E3 embryo water and dechorionated with pronase. Embryos were washed with E3 embryo water, resuspended in blastomere media, inverted  $\sim$ 15 times to dissociate, and filtered through a 40- $\mu$ m nylon mesh filter. Single cells obtained were aliquoted 40  $\mu$ l per well at approximately two embryo equivalents per well and immediately screened with chemicals from the National Institutes of Health (720; Evotec), Library of Pharmacologically Active Compounds (1,440; Sigma), ICCB Known Bioactives (480; Biomol), and Nuclear Hormone Receptor and Kinacore (1,200; ChemBridge) libraries at 30  $\mu$ M. Cells were cultured in a 28°C incubator with 5% CO<sub>2</sub> for 2 d. Cells were stained with draq5 (Cell Signaling Technology) and imaged using a Cell Voyager 7000 (Yokogawa).

A 4 $\times$  image of the nuclear and fluorescent expression from the entire well was then thresholded, and percent area was computed using ImageJ/Fiji. Control wells ( $\geq$ 200 per plate) were identified using quartile exclusion of outliers, and using these wells, a standard curve was built with GFP versus nuclear staining in MatLab. From that standard curve, residuals were calculated for each treated well and divided by the standard deviation in the control wells to obtain the z-score of each chemical treatment.

Dose-response studies using *c-myb:GFP* embryo cultures and follow-up experiments were performed with retinoic acid agonists dissolved in DMSO: AM580 (Tocris), 9-cis retinoic acid (Sigma), retinoic acid p-hydroxyanilide (Sigma), TTNPB (Tocris), AC261066 (Tocris), and ATRA (Sigma).

### Confocal imaging

Double transgenic *c-myb:GFP; lyz:dsRed* (Hall et al., 2007) or *c-myb:GFP; mpeg1:mCherry* (Ellett et al., 2011) embryos from the same clutch were treated between 48 and 72 hpf ( $n = 4$  biological replicates per treatment group) with 10  $\mu$ M ATRA diluted in E3. Live 72-hpf embryos were embedded in 0.8% low-melting point agarose containing 0.04 mg/ml Tricaine and imaged on a Nikon Eclipse Ti microscope with 20 $\times$  Plan-Apo DIC N.A. 0.75. Images

were acquired with Andor iXon x3 EMCCD cameras and NIS Elements software. CHT cells were counted blindly in Z-stack image projections processed on Imaris software (Bitplane). The *c-myb:GFP* cell counts were combined across the two sets and displayed in the graph.

### In situ hybridization

Wild-type AB embryos from the same clutch were treated between 48 and 72 hpf with 10  $\mu$ M retinoic acid agonists diluted in E3, fixed at 72 hpf in 4% paraformaldehyde, and processed as previously described (Thisse and Thisse, 2008). CHT staining in the embryos was blindly scored as high, medium, or low and summed across three independent experiments as done previously (Li et al., 2015). Representative images were acquired on a Nikon ZMS18 microscope.

### Proliferation assays

U937 cells (ATCC) were grown in RPMI 1640 medium (Gibco) supplemented with 10% FBS and 1% penicillin-streptomycin (Gibco) and cultured in a 37°C incubator with 5% CO<sub>2</sub>. U937 cells were tested every other week for mycoplasma contamination using the MycoAlert Mycoplasma Detection Kit (Lonza) and consistently confirmed to be negative. Cells were seeded at an initial density of 1,150 cells/well (96-well plate) with chemicals at the concentrations indicated. After 48 h, cell proliferation rates were determined using a CellTiter-Glo (Promega) luminescent cell viability assay as per the manufacturer's instructions.

### Zebrafish quantitative PCR analysis

Stage-matched 72-hpf *c-myb:GFP* transgenic embryos were finely chopped and dissociated using Liberase (Roche). GFP<sup>+</sup> cells were collected using a FACS Aria cell sorter (BD Biosciences). Sorted cells were resuspended in zebrafish blastomere media and plated with 1  $\mu$ M retinoic acid agonists for 6 h. Cells were then collected and RNA was isolated using the RNeasy Micro Plus Kit (Qiagen) as per the manufacturer's instructions. cDNA was synthesized using the SuperScript III Kit (Life Technologies). Quantitative PCR was performed in triplicate on a Bio-Rad iQ5 real-time PCR machine using Ssofast EvaGreen Supermix (Bio-Rad). Samples were normalized to the  $\beta$ -*actin* gene. The zebrafish primers used were as follows (forward and reverse, respectively): *actin*, 5'-CGA GCAGGAGATGGGAACC-3' and 5'-CAACGGAAACGCTCATTGC-3'; *c-myb*, 5'-TGATGCTTCCCAACACAGAG-3' and 5'-TTCAGAGGG AATCGTCTGCT-3'; *mpx*, 5'-GCTGCTGTGTGCTCTTTCA-3' and 5'-TTGAGTGAGCAGGTTTGTGG-3'; *GFP*, 5'-AAGCTGACCCTGAAG TTCATCTGC-3' and 5'-CTTGTAGTTGCCGTCGTCCTTGAA-3'.

### U937 time course quantitative PCR analysis

U937 cells were plated with 1  $\mu$ M retinoic acid agonists for the duration indicated. Cells were then collected, and RNA was isolated using the RNeasy Plus Mini Kit (Qiagen) as per the manufacturer's instructions. Further processing was done as described in the section above. Samples were normalized to the  $\beta$ -*actin* gene. The human primers used were as follows (forward and reverse, respectively): *actin*, 5'-AGTGGGGTGGCTTTTAGGAT-3' and 5'-CCG AGGACTTTGATTGCACA-3'; *c-myb*, 5'-GGCAGAAATCGCAAAGCT AC-3' and 5'-ACCTTCCTGTTCGACCTTCC-3'.

### Primagraft experiments

For in vivo drug testing, ACC tumor fragments (Moskaluk et al., 2011) from host animals were implanted subcutaneously into the flank of nude mice (CRL: ATH/NU). Once tumors reached 125–250 mm<sup>3</sup>, mice were randomized to receive vehicle or drug diluted in 10:90 DMSO:10% hydroxypropyl- $\beta$ -cyclodextrin orally until controls reached a tumor volume endpoint of 1–2 cm<sup>3</sup> (four to nine mice per group: x5M1 and x6, four treated vs. nine vehicle controls; x9, four treated vs. five vehicle controls; x11, five treated vs. eight vehicle controls). Mice were treated with ATRA (ACC x6 and x11: 4 mg/ml, 0.2 ml-flat dose; ACC x9: 3 mg/ml, 0.2-ml flat dose) or isotretinoin (30 mg/ml, 0.2-ml flat dose). Tumor growth was monitored, and mice were weighed twice weekly; the studies ended when the final group reached tumor volume endpoint. No statistical methods were employed to determine the sample size, and no blinding of investigators was performed. After long-term tumor growth inhibition studies were completed, the ATRA-treated mice stopped receiving treatment and were maintained longer as indicated to monitor tumor maintenance after treatment cessation. The weight data available from two of the three studies are provided. In the ACC x11 model, there was a water bottle issue on day 30, but when treatment was stopped, overall weight gain was noted, and the mice were fine in these two studies. For long-term tumor growth inhibition studies, ACC x6, x9, and x11 models were used, and primagrafts were collected at the completion of the study. Short-term kinetics studies were also undertaken with ACC x9 and x5M1 primagrafts involving 3-d ATRA treatments. All animal procedures used in this study were approved by the IACUC at South Texas Accelerated Research Therapeutics, San Antonio, TX.

### Western blots

ACC x11 (from long-term tumor growth inhibition studies) and ACC x5M1 (from short-term kinetics studies) primagrafts were mechanically homogenized in radioimmunoprecipitation assay lysis buffer (Thermo Scientific) supplemented by the addition of complete protease inhibitor cocktail (Roche). Protein concentrations were determined by detergent compatible protein assay (Bio-Rad). Samples were denatured by adding Laemmli sample buffer (Bio-Rad) with  $\beta$ -mercaptoethanol (Sigma) and boiled at 95°C for 5 min. 10  $\mu$ g of protein was resolved by electrophoresis through 4–20% mini-PROTEAN TGX (Bio-Rad) precast gels. Proteins were transferred onto a nitrocellulose membrane using the iBlot dry blotting system (Invitrogen). Membranes were incubated overnight with the following primary antibodies: anti-Myb (ab45150; Abcam), anti-RAR $\alpha$  (MAB5346; Chemicon), and anti-GAPDH (2118s; Cell Signaling Technology) as loading control. Protein bands were detected using horse anti-mouse HRP (7076S; Cell Signaling Technology) or goat anti-rabbit HRP (7074S; Cell Signaling Technology). Three biological replicates (individual primagrafts from different mice) for each treatment group were analyzed for protein expression. HEK293T cell lysate, which lacks MYB expression, was processed similarly and used as a negative control on the same blots.

### Immunohistochemistry

Sectioning and staining was performed by the Dana-Farber/Harvard Cancer Center Specialized Histopathology Core using

standard procedures on ACC x6, x9, and x11 samples (from long-term tumor growth inhibition studies). Slides were baked for 60 min in an oven set to 60°C and loaded into the Bond III staining platform with appropriate labels. Slides were either antigen retrieved in Bond Epitope Retrieval 2 for 20 min and incubated with Ki-67 (SP6) (CRM325; Biocare) at 1:200 for 30 min at room temperature, or antigen-retrieved in Bond Epitope Retrieval 1 for 30 min and incubated with cleaved caspase-3 (5A1E; 9664; Cell Signaling Technology) at 1:150 for 30 min at room temperature. Primary antibody was detected using the Bond Polymer Refine Detection Kit. Slides were developed in 3,3'-diaminobenzidine, dehydrated, and coverslipped. Transmitted light images were acquired on a Nikon Eclipse E600 microscope at 40 $\times$ . Images (>200 nuclei each) from three different individual primagrafts were blindly quantitated.

### RNA-seq and bioinformatics

RNA-seq was performed on three biological replicates of ACC x9 primagrafts (from short-term kinetics studies) treated with vehicle or ATRA for 3 d (individual primagrafts from different mice). Frozen primagrafts were lysed, and RNA was isolated using the RNeasy Mini Plus Kit (Qiagen) as per the manufacturer's instructions. Ribosomal RNA was then depleted using the Ribo-Zero Gold Kit (Epicentre) as per the manufacturer's instructions. Sequencing libraries were constructed from ribosome-depleted RNA samples using the NEBNext Ultra Kit (New England Biolabs) and sequenced on a Hi-Seq 2500 instrument (Illumina).

Quality control of RNA-seq datasets was performed by FastQC and Cutadapt to remove adaptor sequences and low quality regions. The high quality reads were aligned to the University of California, Santa Cruz (UCSC) Genome Browser build hg19 of the human genome using Tophat 2.0.11 without novel splicing form calls. Transcript abundance and differential expression were calculated with Cufflinks 2.2.1. FPKM (fragments per kilobase of exon per million fragments mapped) values were used to normalize and quantify each transcript; the resulting list of differential expressed genes were filtered by log fold change >2 and *q*-value <0.05. Datasets are deposited in the Gene Expression Omnibus under accession no. GSE98008.

### ChIP-seq and bioinformatics

ChIP-seq was performed on ACC x9 primagrafts (from short-term kinetics studies) treated with vehicle or ATRA for 3 d. Frozen primagrafts were mechanically dissociated, formaldehyde cross-linked, and collected. ChIP was performed as described previously (Lee et al., 2006) with 10  $\mu$ g of antibodies against *c-myb* (A304-136A; Bethyl), pan-RAR (sc-773X; Santa Cruz), and H3K27ac (ab4729; Abcam). Sequencing libraries were constructed using the NEBNext Multiplex Oligos Kit (New England Biolabs) and sequenced on a Hi-Seq 2500 instrument (Illumina).

All ChIP-seq datasets were aligned to UCSC build version hg19 of the human genome using Bowtie2 (version 2.2.1; Langmead and Salzberg, 2012) with the following parameters: -end-to-end, -NO, -L20. We used the MACS2 version 2.1.0 (Zhang et al., 2008) peak-finding algorithm to identify regions of ChIP-seq peaks, with a 0.05 *q*-value threshold of enrichment for all datasets. ChIP-seq enrichment was determined as described previously

(Trompouki et al., 2011) in a 5-kb region (as counts per million) centered on the enriched peak regions ( $n = 1,872$ ) of the given MYB datasets. Datasets are deposited in the Gene Expression Omnibus under accession no. GSE98008.

Heat maps of the ChIP-seq binding were generated using the input normalized results of the MACS peak calling output. The outputted bedGraph files were converted to BigWig files. Those files were then processed using computeMatrix and plotHeatmap tools within the deeptools 3.0 package. All figures centered on called peaks from the macs2 output. Those peaks were assigned genes using GREAT to find genes within 15 kb of peaks. The peaks that had genes that had an associated fold change of 1.2 by RNA-seq were extracted and used to generate further figures.

Super-enhancers were identified as previously described (Hnisz et al., 2013). H3K27ac peaks from vehicle-treated ACC primagrafts were used to locate enhancers, and H3K27ac signal minus the input control was used to rank enhancers based on enrichment.

### Statistics

As previously described (Li et al., 2015), in situ hybridization experiments were analyzed by  $\chi^2$  or Fisher's exact test if sample sizes were small. All other *P* values were determined by unpaired two-tailed Student's *t* test by comparing treated samples to untreated controls. Significance of dose-response curves and proliferation assays was determined at a 1  $\mu$ M concentration. Significance of ATRA or isotretinoin treatment in the long-term primagraft experiments was determined by comparing the change in tumor growth in the control and treated groups. Statistics were performed using GraphPad Prism software. Graphs show means with SEM as indicated.

### Data and materials availability

ChIP-seq and RNA-seq data have been deposited in the Gene Expression Omnibus (accession no. GSE98008).

### Online supplemental material

Fig. S1 shows how retinoic acid agonists down-regulated *c-myb:GFP* in dose-response curves. Fig. S2 shows how ATRA decreased *c-myb*-positive cells in vivo in the CHT of zebrafish embryos. Fig. S3 shows how retinoic acid agonists down-regulated *c-myb* expression in human U937 cells. Fig. S4 shows tumor maintenance curves after ATRA was discontinued in ACC xenotransplants and the percent weight change of the mice. Fig. S5 shows ATRA down-regulated MYB levels in short-term ACC primagrafts, and immunohistochemistry images of primagrafts. Table S1 lists the hits we identified in our screen of chemical down-regulators of *c-myb:GFP* zebrafish embryo cultures that maintained normal embryoid body formation. Table S2 lists the ranked super-enhancers in ACC primagrafts and associated genes.

### Acknowledgments

We thank Y. Zhou, S. Yang, A. Lichtig, R. Mathieu, and T. Schlaeger for technical assistance and J. Aster, E. Hagedorn, and R. Young for helpful discussions. FACS was performed by the Boston Children's Hospital Flow Cytometry Research Facility Core.

Immunohistochemistry was performed by the Dana-Farber/Harvard Cancer Center Specialized Histopathology Core.

This work was supported by the Adenoid Cystic Carcinoma Research Foundation; the Harvard Stem Cell Institute; the Howard Hughes Medical Institute; National Institutes of Health grants R01 HL048801, P01 HL032262, P30 DK049216, R01 DK053298, U01 HL100001, and R24 DK092760 to L.I. Zon; the Canadian Institutes of Health Research Doctoral Foreign Study Award DFS-146184 to J. Mandelbaum; and the American Cancer Society Postdoctoral Fellowship 122577PF1214601DDC to I.A. Shestopalov.

L.I. Zon is a founder and stockholder of Fate Therapeutics, Scholar Rock, and CAMP4 Therapeutics. The authors declare no other competing financial interests.

Author contributions: L.I. Zon, J. Mandelbaum, and I.A. Shestopalov designed the study. J. Mandelbaum, I.A. Shestopalov, R.E. Henderson, B. Knoechel, and M.J. Wick performed experiments, analyzed data, and gave conceptual advice. L.I. Zon, J. Mandelbaum, and N.G. Chau wrote the manuscript. All authors discussed the results and reviewed the manuscript.

Submitted: 21 May 2018

Revised: 16 July 2018

Accepted: 23 August 2018

## References

- Allenby, G., M.T. Bocquel, M. Saunders, S. Kazmer, J. Speck, M. Rosenberger, A. Lovey, P. Kastner, J.F. Grippo, P. Chambon, et al. 1993. Retinoic acid receptors and retinoid X receptors: interactions with endogenous retinoic acids. *Proc. Natl. Acad. Sci. USA.* 90:30–34. <https://doi.org/10.1073/pnas.90.1.30>
- Almeida, L.O., D.M. Guimarães, M.D. Martins, M.A.T. Martins, K.A. Warner, J.E. Nör, R.M. Castilho, and C.H. Squarize. 2017. Unlocking the chromatin of adenoid cystic carcinomas using HDAC inhibitors sensitize cancer stem cells to cisplatin and induces tumor senescence. *Stem Cell Res. (Amst.)*. 21:94–105. <https://doi.org/10.1016/j.scr.2017.04.003>
- Bobbio, A., C. Copelli, L. Ampollini, B. Bianchi, P. Carbognani, S. Bettati, E. Sesenna, and M. Rusca. 2008. Lung metastasis resection of adenoid cystic carcinoma of salivary glands. *Eur. J. Cardiothorac. Surg.* 33:790–793. <https://doi.org/10.1016/j.ejcts.2007.12.057>
- Boise, L.H., K.M. Gorse, and E.H. Westin. 1992. Multiple mechanisms of regulation of the human c-myc gene during myelomonocytic differentiation. *Oncogene*. 7:1817–1825.
- Bradley, P.J. 2004. Adenoid cystic carcinoma of the head and neck: a review. *Curr. Opin. Otolaryngol. Head Neck Surg.* 12:127–132. <https://doi.org/10.1097/00020840-200404000-00013>
- Brayer, K.J., C.A. Frerich, H. Kang, and S.A. Ness. 2016. Recurrent Fusions in MYB and MYBL1 Define a Common, Transcription Factor-Driven Oncogenic Pathway in Salivary Gland Adenoid Cystic Carcinoma. *Cancer Discov.* 6:176–187. <https://doi.org/10.1158/2159-8290.CD-15-0859>
- Bruinsma, W., J.A. Raaijmakers, and R.H. Medema. 2012. Switching Polo-like kinase-1 on and off in time and space. *Trends Biochem. Sci.* 37:534–542. <https://doi.org/10.1016/j.tibs.2012.09.005>
- Coca-Pelaz, A., J.P. Rodrigo, P.J. Bradley, V. Vander Poorten, A. Triantafyllou, J.L. Hunt, P. Strojjan, A. Rinaldo, M. Haigentz Jr., R.P. Takes, et al. 2015. Adenoid cystic carcinoma of the head and neck—An update. *Oral Oncol.* 51:652–661. <https://doi.org/10.1016/j.oraloncology.2015.04.005>
- Cohen, D.E., and D. Melton. 2011. Turning straw into gold: directing cell fate for regenerative medicine. *Nat. Rev. Genet.* 12:243–252. <https://doi.org/10.1038/nrg2938>
- Conley, J., and D.L. Dingman. 1974. Adenoid cystic carcinoma in the head and neck (cylindroma). *Arch. Otolaryngol.* 100:81–90. <https://doi.org/10.1001/archotol.1974.00780040087001>
- Cunningham, T.J., and G. Duester. 2015. Mechanisms of retinoic acid signaling and its roles in organ and limb development. *Nat. Rev. Mol. Cell Biol.* 16:110–123. <https://doi.org/10.1038/nrm3932>
- Das, B.C., P. Thapa, R. Karki, S. Das, S. Mahapatra, T.C. Liu, I. Torregroza, D.P. Wallace, S. Kambhampati, P. Van Veldhuizen, et al. 2014. Retinoic acid signaling pathways in development and diseases. *Bioorg. Med. Chem.* 22:673–683. <https://doi.org/10.1016/j.bmc.2013.11.025>
- Degos, L., and Z.Y. Wang. 2001. All trans retinoic acid in acute promyelocytic leukemia. *Oncogene*. 20:7140–7145. <https://doi.org/10.1038/sj.onc.1204763>
- Drier, Y., M.J. Cotton, K.E. Williamson, S.M. Gillespie, R.J. Ryan, M.J. Kluk, C.D. Carey, S.J. Rodig, L.M. Sholl, A.H. Afrogheh, et al. 2016. An oncogenic MYB feedback loop drives alternate cell fates in adenoid cystic carcinoma. *Nat. Genet.* 48:265–272. <https://doi.org/10.1038/ng.3502>
- Ellett, F., L. Pase, J.W. Hayman, A. Adrianopoulos, and G.J. Lieschke. 2011. mpeg1 promoter transgenes direct macrophage-lineage expression in zebrafish. *Blood*. 117:e49–e56. <https://doi.org/10.1182/blood-2010-10-314120>
- Evans, R.M., and D.J. Mangelsdorf. 2014. Nuclear Receptors, RXR, and the Big Bang. *Cell*. 157:255–266. <https://doi.org/10.1016/j.cell.2014.03.012>
- Ferrarotto, R., Y. Mitani, L. Diao, I. Guijarro, J. Wang, P. Zweidler-McKay, D. Bell, W.N. William Jr., B.S. Glisson, M.J. Wick, et al. 2017. Activating NOTCH1 Mutations Define a Distinct Subgroup of Patients With Adenoid Cystic Carcinoma Who Have Poor Prognosis, Propensity to Bone and Liver Metastasis, and Potential Responsiveness to Notch1 Inhibitors. *J. Clin. Oncol.* 35:352–360. <https://doi.org/10.1200/JCO.2016.67.5264>
- Graf, T. 1992. Myb: a transcriptional activator linking proliferation and differentiation in hematopoietic cells. *Curr. Opin. Genet. Dev.* 2:249–255. [https://doi.org/10.1016/S0959-437X\(05\)80281-3](https://doi.org/10.1016/S0959-437X(05)80281-3)
- Hall, C., M.V. Flores, T. Storm, K. Crosier, and P. Crosier. 2007. The zebrafish lysozyme C promoter drives myeloid-specific expression in transgenic fish. *BMC Dev. Biol.* 7:42. <https://doi.org/10.1186/1471-213X-7-42>
- Hickman, R.E., R.A. Cawson, and S.W. Duffy. 1984. The prognosis of specific types of salivary gland tumors. *Cancer*. 54:1620–1624. [https://doi.org/10.1002/1097-0142\(19841015\)54:8%3C1620::AID-CNCR2820540824%3E3.O.CO;2-I](https://doi.org/10.1002/1097-0142(19841015)54:8%3C1620::AID-CNCR2820540824%3E3.O.CO;2-I)
- Hnisz, D., B.J. Abraham, T.I. Lee, A. Lau, V. Saint-André, A.A. Sigova, H.A. Hoke, and R.A. Young. 2013. Super-enhancers in the control of cell identity and disease. *Cell*. 155:934–947. <https://doi.org/10.1016/j.cell.2013.09.053>
- Ho, A.S., K. Kannan, D.M. Roy, L.G. Morris, I. Ganly, N. Katabi, D. Ramaswami, L.A. Walsh, S. Eng, J.T. Huse, et al. 2013. The mutational landscape of adenoid cystic carcinoma. *Nat. Genet.* 45:791–798. <https://doi.org/10.1038/ng.2643>
- Langmead, B., and S.L. Salzberg. 2012. Fast gapped-read alignment with Bowtie 2. *Nat. Methods*. 9:357–359. <https://doi.org/10.1038/nmeth.1923>
- Lee, T.I., S.E. Johnstone, and R.A. Young. 2006. Chromatin immunoprecipitation and microarray-based analysis of protein location. *Nat. Protoc.* 1:729–748. <https://doi.org/10.1038/nprot.2006.98>
- Li, P., J.L. Lahvic, V. Binder, E.K. Pugach, E.B. Riley, O.J. Tamplin, D. Panigrahy, T.V. Bowman, F.G. Barrett, G.C. Heffner, et al. 2015. Epoxyeicosatrienoic acids enhance embryonic haematopoiesis and adult marrow engraftment. *Nature*. 523:468–471. <https://doi.org/10.1038/nature14569>
- Lo-Coco, F., L. Di Donato, R.F. Schlenk, GIMEMA, and German-Austrian Acute Myeloid Leukemia Study Group and Study Alliance Leukemia. 2016. Targeted Therapy Alone for Acute Promyelocytic Leukemia. *N. Engl. J. Med.* 374:1197–1198. <https://doi.org/10.1056/NEJMc1513710>
- Lutz, P.G., A. Houzel-Charavel, C. Moog-Lutz, and Y.E. Cayre. 2001. Myeloblastin is an Myb target gene: mechanisms of regulation in myeloid leukemia cells growth-arrested by retinoic acid. *Blood*. 97:2449–2456. <https://doi.org/10.1182/blood.V97.8.2449>
- Mathelier, A., O. Fornes, D.J. Arenillas, C.Y. Chen, G. Denay, J. Lee, W. Shi, C. Shyr, G. Tan, R. Worsley-Hunt, et al. 2016. JASPAR 2016: a major expansion and update of the open-access database of transcription factor binding profiles. *Nucleic Acids Res.* 44(D1):D110–D115. <https://doi.org/10.1093/nar/gkv1176>
- McKeown, M.R., M.R. Corces, M.L. Eaton, C. Fiore, E. Lee, J.T. Lopez, M.W. Chen, D. Smith, S.M. Chan, J.L. Koenig, et al. 2017. Superenhancer Analysis Defines Novel Epigenomic Subtypes of Non-APL AML, Including an RARα Dependency Targetable by SY-1425, a Potent and Selective RARα Agonist. *Cancer Discov.* 7:1136–1153. <https://doi.org/10.1158/2159-8290.CD-17-0399>
- Mikse, O.R., J.H. Tchaicha, E.A. Akbay, L. Chen, R.T. Bronson, P.S. Hammerman, and K.K. Wong. 2016. The impact of the MYB-NFIB fusion proto-oncogene in vivo. *Oncotarget*. 7:31681–31688. <https://doi.org/10.18632/oncotarget.9426>
- Mitani, Y., B. Liu, P.H. Rao, V.J. Borra, M. Zafereo, R.S. Weber, M. Kies, G. Lozano, P.A. Futreal, C. Caulin, and A.K. El-Naggar. 2016. Novel MYBL1

- Gene Rearrangements with Recurrent MYBL1-NFIB Fusions in Salivary Adenoid Cystic Carcinomas Lacking t(6;9) Translocations. *Clin. Cancer Res.* 22:725–733. <https://doi.org/10.1158/1078-0432.CCR-15-2867-T>
- Moskaluk, C.A., A.S. Baras, S.A. Mancuso, H. Fan, R.J. Davidson, D.C. Dirks, W.L. Golden, and H.F. Frierson Jr. 2011. Development and characterization of xenograft model systems for adenoid cystic carcinoma. *Lab. Invest.* 91:1480–1490. <https://doi.org/10.1038/labinvest.2011.105>
- Nör, F., K.A. Warner, Z. Zhang, G.A. Acasigua, A.T. Pearson, S.A. Kerck, J.I. Helman, M. Sant'Ana Filho, S. Wang, and J.E. Nör. 2017. Therapeutic Inhibition of the MDM2-p53 Interaction Prevents Recurrence of Adenoid Cystic Carcinomas. *Clin. Cancer Res.* 23:1036–1048. <https://doi.org/10.1158/1078-0432.CCR-16-1235>
- North, T.E., W. Goessling, C.R. Walkley, C. Lengerke, K.R. Kopani, A.M. Lord, G.J. Weber, T.V. Bowman, I.H. Jang, T. Grosser, et al. 2007. Prostaglandin E2 regulates vertebrate haematopoietic stem cell homeostasis. *Nature.* 447:1007–1011. <https://doi.org/10.1038/nature05883>
- O'Farrell, P.H. 2001. Triggering the all-or-nothing switch into mitosis. *Trends Cell Biol.* 11:512–519. [https://doi.org/10.1016/S0962-8924\(01\)02142-0](https://doi.org/10.1016/S0962-8924(01)02142-0)
- Oh, I.H., and E.P. Reddy. 1999. The myb gene family in cell growth, differentiation and apoptosis. *Oncogene.* 18:3017–3033. <https://doi.org/10.1038/sj.onc.1202839>
- Olsson, I.L., and T.R. Breitman. 1982. Induction of differentiation of the human histiocytic lymphoma cell line U-937 by retinoic acid and cyclic adenosine 3'-5'-monophosphate-inducing agents. *Cancer Res.* 42:3924–3927.
- Orkin, S.H., and L.I. Zon. 2008. Hematopoiesis: an evolving paradigm for stem cell biology. *Cell.* 132:631–644. <https://doi.org/10.1016/j.cell.2008.01.025>
- Ottewill, P.D., D.V. Lefley, S.S. Cross, C.A. Evans, R.E. Coleman, and I. Holen. 2010. Sustained inhibition of tumor growth and prolonged survival following sequential administration of doxorubicin and zoledronic acid in a breast cancer model. *Int. J. Cancer.* 126:522–532. <https://doi.org/10.1002/ijc.24756>
- Panaccione, A., Y. Zhang, M. Ryan, C.A. Moskaluk, K.S. Anderson, W.G. Yarbrough, and S.V. Ivanov. 2017. MYB fusions and CD markers as tools for authentication and purification of cancer stem cells from salivary adenoid cystic carcinoma. *Stem Cell Res. (Amst.)*. 21:160–166. <https://doi.org/10.1016/j.scr.2017.05.002>
- Persson, M., Y. Andrén, J. Mark, H.M. Horlings, F. Persson, and G. Stenman. 2009. Recurrent fusion of MYB and NFIB transcription factor genes in carcinomas of the breast and head and neck. *Proc. Natl. Acad. Sci. USA.* 106:18740–18744. <https://doi.org/10.1073/pnas.0909114106>
- Pfitzner, E., J. Kirfel, P. Becker, A. Rolke, and R. Schüle. 1998. Physical interaction between retinoic acid receptor and the oncoprotein myb inhibits retinoic acid-dependent transactivation. *Proc. Natl. Acad. Sci. USA.* 95:5539–5544. <https://doi.org/10.1073/pnas.95.10.5539>
- Ramsay, R.G., and T.J. Gonda. 2008. MYB function in normal and cancer cells. *Nat. Rev. Cancer.* 8:523–534. <https://doi.org/10.1038/nrc2439>
- Rivera, C.M., and B. Ren. 2013. Mapping human epigenomes. *Cell.* 155:39–55. <https://doi.org/10.1016/j.cell.2013.09.011>
- Ross, J.S., K. Wang, J.V. Rand, C.E. Sheehan, T.A. Jennings, R.N. Al-Rohil, G.A. Otto, J.C. Curran, G. Palmer, S.R. Downing, et al. 2014. Comprehensive genomic profiling of relapsed and metastatic adenoid cystic carcinomas by next-generation sequencing reveals potential new routes to targeted therapies. *Am. J. Surg. Pathol.* 38:235–238. <https://doi.org/10.1097/PAS.000000000000102>
- Ruggeri, B.A., F. Camp, and S. Miknyoczki. 2014. Animal models of disease: pre-clinical animal models of cancer and their applications and utility in drug discovery. *Biochem. Pharmacol.* 87:150–161. <https://doi.org/10.1016/j.bcp.2013.06.020>
- Seethala, R.R. 2009. An update on grading of salivary gland carcinomas. *Head Neck Pathol.* 3:69–77. <https://doi.org/10.1007/s12105-009-0102-9>
- Shepard, J.L., J.F. Amatruda, H.M. Stern, A. Subramanian, D. Finkelstein, J. Ziai, K.R. Finley, K.L. Pfaff, C. Hersey, Y. Zhou, et al. 2005. A zebrafish bmyb mutation causes genome instability and increased cancer susceptibility. *Proc. Natl. Acad. Sci. USA.* 102:13194–13199. <https://doi.org/10.1073/pnas.0506583102>
- Smarda, J., J. Sugarman, C. Glass, and J. Lipsick. 1995. Retinoic acid receptor alpha suppresses transformation by v-myb. *Mol. Cell. Biol.* 15:2474–2481. <https://doi.org/10.1128/MCB.15.5.2474>
- Spiro, R.H. 1997. Distant metastasis in adenoid cystic carcinoma of salivary origin. *Am. J. Surg.* 174:495–498. [https://doi.org/10.1016/S0002-9610\(97\)00153-0](https://doi.org/10.1016/S0002-9610(97)00153-0)
- Stephens, P.J., H.R. Davies, Y. Mitani, P. Van Loo, A. Shlien, P.S. Tarpey, E. Papaemmanuil, A. Cheverton, G.R. Bignell, A.P. Butler, et al. 2013. Whole exome sequencing of adenoid cystic carcinoma. *J. Clin. Invest.* 123:2965–2968. <https://doi.org/10.1172/JCI67201>
- Stoeck, A., S. Lejnine, A. Truong, L. Pan, H. Wang, C. Zang, J. Yuan, C. Ware, J. MacLean, P.W. Garrett-Engele, et al. 2014. Discovery of biomarkers predictive of GSI response in triple-negative breast cancer and adenoid cystic carcinoma. *Cancer Discov.* 4:1154–1167. <https://doi.org/10.1158/2159-8290.CD-13-0830>
- Subramanian, A., P. Tamayo, V.K. Mootha, S. Mukherjee, B.L. Ebert, M.A. Gillette, A. Paulovich, S.L. Pomeroy, T.R. Golub, E.S. Lander, and J.P. Mesirov. 2005. Gene set enrichment analysis: a knowledge-based approach for interpreting genome-wide expression profiles. *Proc. Natl. Acad. Sci. USA.* 102:15545–15550. <https://doi.org/10.1073/pnas.0506580102>
- Thiele, C.J., P.S. Cohen, and M.A. Israel. 1988. Regulation of c-myb expression in human neuroblastoma cells during retinoic acid-induced differentiation. *Mol. Cell. Biol.* 8:1677–1683. <https://doi.org/10.1128/MCB.8.4.1677>
- Thisse, C., and B. Thisse. 2008. High-resolution in situ hybridization to whole-mount zebrafish embryos. *Nat. Protoc.* 3:59–69. <https://doi.org/10.1038/nprot.2007.514>
- Thompson, M.A., and R.G. Ramsay. 1995. Myb: an old oncoprotein with new roles. *BioEssays.* 17:341–350. <https://doi.org/10.1002/bies.950170410>
- Trompouki, E., T.V. Bowman, L.N. Lawton, Z.P. Fan, D.C. Wu, A. DiBiase, C.S. Martin, J.N. Cech, A.K. Sessa, J.L. Leblanc, et al. 2011. Lineage regulators direct BMP and Wnt pathways to cell-specific programs during differentiation and regeneration. *Cell.* 147:577–589. <https://doi.org/10.1016/j.cell.2011.09.044>
- van Weert, S., I. van der Waal, B.I. Witte, C.R. Leemans, and E. Bloemena. 2015. Histopathological grading of adenoid cystic carcinoma of the head and neck: analysis of currently used grading systems and proposal for a simplified grading scheme. *Oral Oncol.* 51:71–76. <https://doi.org/10.1016/j.oraloncology.2014.10.007>
- Wang, G., Q. Jiang, and C. Zhang. 2014. The role of mitotic kinases in coupling the centrosome cycle with the assembly of the mitotic spindle. *J. Cell Sci.* 127:4111–4122. <https://doi.org/10.1242/jcs.151753>
- Weston, K.M. 1990. The myb genes. *Semin. Cancer Biol.* 1:371–382.
- Wysocki, P.T., E. Izumchenko, J. Meir, P.K. Ha, D. Sidransky, and M. Brait. 2016. Adenoid cystic carcinoma: emerging role of translocations and gene fusions. *Oncotarget.* 7:66239–66254. <https://doi.org/10.18632/oncotarget.11288>
- Xu, C., M. Tabebordbar, S. Iovino, C. Ciarlo, J. Liu, A. Castiglioni, E. Price, M. Liu, E.R. Barton, C.R. Kahn, et al. 2013. A zebrafish embryo culture system defines factors that promote vertebrate myogenesis across species. *Cell.* 155:909–921. <https://doi.org/10.1016/j.cell.2013.10.023>
- Yarbrough, W.G., A. Panaccione, M.T. Chang, and S.V. Ivanov. 2016. Clinical and molecular insights into adenoid cystic carcinoma: Neural crest-like stemness as a target. *Laryngoscope Investig. Otolaryngol.* 1:60–77. <https://doi.org/10.1002/lio2.22>
- Zemanová, K., and J. Smarda. 1998. Oncoprotein v-Myb and retinoic acid receptor alpha are mutual antagonists. *Blood Cells Mol. Dis.* 24:239–250. <https://doi.org/10.1006/bcmd.1998.0189>
- Zhang, Y., T. Liu, C.A. Meyer, J. Eeckhoutte, D.S. Johnson, B.E. Bernstein, C. Nusbaum, R.M. Myers, M. Brown, W. Li, and X.S. Liu. 2008. Model-based analysis of ChIP-Seq (MACS). *Genome Biol.* 9:R137. <https://doi.org/10.1186/gb-2008-9-9-r137>